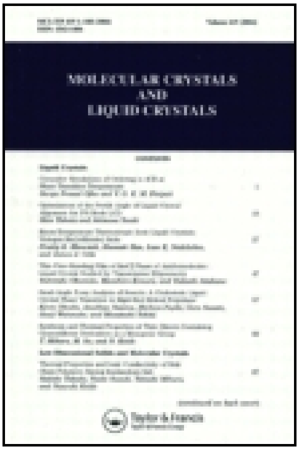

Molecular Crystals and Liquid Crystals
Publication details, including instructions for authors and subscription information:
http://www.tandfonline.com/loi/gmcl16

Absorption, Fluorescence and Phosphorescence Spectra of Hexachlorobenzene Single Crystals at 4.2°K

G. A. George [a] [b] & G. C. Morris [a]
[a] Department of Chemistry, University of Queensland, St. Lucia, 4067, Queensland
[b] Department of Supply (Aust.) Student

Version of record first published: 08 Dec 2010.

To cite this article: G. A. George & G. C. Morris (1970): Absorption, Fluorescence and Phosphorescence Spectra of Hexachlorobenzene Single Crystals at 4.2°K, Molecular Crystals and Liquid Crystals, 10:1-2, 187-217

To link to this article: http://dx.doi.org/10.1080/15421407008083494

Molecular Crystals and Liquid Crystals. 1970. Vol. 10, 187–217

Printed in Great Britain

Absorption, Fluorescence and Phosphorescence Spectra of Hexachlorobenzene Single Crystals at 4.2 °K

G. A. GEORGE† and G. C. MORRIS

Department of Chemistry
University of Queensland
St. Lucia, 4067
Queensland

Received February 16, 1970

Abstract—The low lying singlet and triplet states of high purity single crystals of hexachlorobenzene are investigated. The fluorescence quantum yield is 10^{-2}. The polarized fluorescence spectrum at 4.2 °K is analyzed as a pure exciton emission. There is no evidence for emission from trap levels. The electronic origin for the first singlet transition is at 32736 cm^{-1}.

The phosphorescence quantum yield is 10^{-2}. The triplet exciton emission origin is at 25685 cm^{-1} which coincides with the direct triplet exciton absorption origin in contrast to other reports. The crystal phosphorescence is very sensitive to crystal temperature between 4.2 and 15 °K. At 4.2 °K the emission origin is 39 cm^{-1} below the triplet exciton band. Emission from the triplet exciton band is observed when the crystal temperature is above 4.2 °K. The spectrum is interpreted in terms of a low lying trap level due presumably to impurity induced displacement of the triplet energy level of some hexachlorobenzene molecules and a deep lying trap (1345 cm^{-1}) which at high temperatures acts as the main emitting centre.

The polarized $S_0 \rightarrow T_1$ and $S_0 \rightarrow T_2$ absorption spectra are observed. The second triplet exciton origin is at 32240 cm^{-1}. The presence of in-plane intensity in the $S_0 \rightarrow T_1$ absorption spectrum suggests that the molecular symmetry is not D_{6h} in the triplet state.

1. Introduction

The crystals of halogenated benzene molecules are of particular interest for studies of the triplet state.$^{(1,2)}$ Significant spin–orbit

---

† Department of Supply (Aust.) Student.

coupling for aromatic π-electrons associated with the heavy atom results in

(i) a marked decrease of the triplet exciton lifetime compared with benzene so that pure exciton phosphorescence may be observed from crystals at 4.2 °K;

(ii) enhancement, compared with benzene, of the $S_0 \rightarrow T_1$ transition probability so that high resolution polarized absorption spectra and Zeeman effect studies(3) may be carried out for this transition. In particular, Castro and Hochstrasser(1,2,3) have reported on the spatial symmetry and distortions of the triplet state molecule, the extent and type of spin–orbit and spin–vibronic coupling, the triplet exciton band width and the crystal field effects for the *p*-dihalogenated benzenes.

There have been conflicting reports on the value of the transition energy for the transition $S_0 \rightarrow T_1$ of hexachlorobenzene (HCB). Phosphorescence of hexachlorobenzene in a frozen glass at 90 °K was first reported by Kasha.(4) The emission origin was at 24170 cm^{-1}. In a crystal at 20 °K, a structured phosphorescence spectrum was obtained by Pesteil *et al.*(5) with an emission origin at 22574 cm^{-1}. Zmerli and Pesteil(6) reinvestigated the phosphorescence at 90 °K and found an emission whose origin was at 24350 cm^{-1}, i.e. blue shifted by $\sim 1800\ \text{cm}^{-1}$ from the 20 °K origin. Olds(7) reported polarized phosphorescence from the crystal at 77 °K with an origin at 24322 cm^{-1}, in agreement with Zmerli and Pesteil.(6) Russell and Albrecht(8) using a frozen 3-methyl pentane solution of hexachlorobenzene at 77 °K observed a structureless emission with a broad maximum around 19500 cm^{-1}. The only published $S_0 \rightarrow T_1$ absorption spectrum is a phosphorescence excitation spectrum of a naphthalene doped crystal at 77 °K.(9) The origin was placed at 25640 cm^{-1}.

The large separation between the origin of crystal(7) and frozen solution(8) phosphorescence is not explicable in terms of environmental shift of the transition energy of the triplet state. The shift on passing from solution to the crystal depends largely on the sum over the crystal of the interaction energy between translationally equivalent molecules together with the factor group splitting resulting from coupling between inequivalent molecules.(10) For the singlet state, the terms are coulombic only and the shift depends on the oscillator strength of the electronic transition. In the triplet state, electron exchange integrals are considered together with any coulombic contributions resulting from spin–orbit coupling. These terms should provide only minor contributions in comparison, say, with the shift for the transition energy of the singlet state. For anthracene, the transition energy of the singlet state shifts by 1350 cm^{-1} from a solid matrix to the crystal,(11) but the transition energy of the triplet state shifts by less than 100 cm^{-1}.(12)

The reported phosphorescence spectrum of the hexachlorobenzene crystal at 77 °K shows a red shift of $\sim$1300 cm^{-1} from the origin of the $S_0 \rightarrow T_1$ absorption spectrum of a naphthalene-doped crystal. Ron and Schnepp, in unpublished work (quoted by Marchetti and Kearns(8)), report a $S_0 \rightarrow T_1$ origin obtained by direct crystal absorption that agrees to within experimental error (± 5 Å) with the doped crystal origin. The observation of a shift between absorption and emission for a molecule which shows substantial vibrational structure is unexpected. We note for example, that the origin bands of the phosphorescence and singlet-triplet absorption spectra of the *p*-dihalogenated benzenes coincide.(1) Unless there is a significant conformational change of the molecule following excitation a red shift of the magnitude observed for hexachlorobenzene (1300 cm^{-1}) is unexpected.

From the crystal phosphorescence studies of Pesteil *et al.*,(5,6) the shift of 1500 cm^{-1} on cooling from 90 °K to 20 °K is difficult to interpret other than as energy trapping in the crystal by impurities with lower lying electronic energy levels. Traces of impurity in concentrations as low as one part in 10^6 can result in an emission spectrum characteristic of the guest (impurity) molecule.(10) Since none of the above studies was carried out on ultra pure hexachlorobenzene, it is likely that impurity effects are dominating the previously published phosphorescence emission spectra. Whether this is true of the singlet emission is uncertain. No fluorescence has been observed from the crystal at either 77 °K or 4 °K.(13)

In the course of our investigations of electronic energy transfer and relaxation in molecular crystals, we have investigated the low lying singlet and triplet states of high purity single crystals of hexachlorobenzene. Fluorescence, phosphorescence, and $S_0 \rightarrow T_1$ and $S_0 \rightarrow T_2$ absorption are reported.

2. Experimental

Hexachlorobenzene (B.D.H. Organic Analytical Standard grade) was recrystallized twice from A.R. chloroform, chromatographed over alumina and vacuum sublimed. This material was then zone refined for fifty passes under a pressure of 1 cm Hg of purified nitrogen. The central fraction was transferred to a second tube and zone refined for one hundred passes. The central fraction of this was transferred to a crystal growth tube. All handling was carried out under vacuum of about 10^{-5} mm Hg and under yellow light. Crystals were melt grown in a Bridgman furnace. The principal cleavage was found to be (001). Samples could also be cleaved along the secondary cleavage plane (100).

Crystals were mounted in a liquid helium cryostat and the temperature was monitored by a Germanium resistance thermometer. Fluorescence and phosphorescence were excited by 265 nm radiation filtered from a 1600 V.A. Xenon arc by a filter consisting of 5 cm of $NiSO_4/CoSO_4$ solution, 5 cm of purified chlorine gas at 1 atmosphere and a Corning CS7–54 filter. The weak crystal emission was analyzed by a Spex 1702, 0.75 m spectrometer, f/6.8, with grating 1200 lines/mm blazed at 3000 Å. Spectra were recorded photographically on Kodak TRI-X film or photoelectrically with an EMI 6256S photomultiplier and either electrometer amplification or phase sensitive detection. Spectra were calibrated with iron and mercury arcs. Polaroid HNP'B was used as a UV polarizer. Singlet-triplet absorption spectra were obtained by phosphorescence excitation.(14) The low light intensities involved have restricted our studies to an equivalent slit width of 4 cm^{-1}. Absolute crystal quantum yields were measured at 77 °K by using a liquid nitrogen cryostat in which a diffuse reflector ($BaSO_4$) could be rotated into the place of the sample. Excitation and analyzing monochromators were 0.25 m Jarrell–Ash, f/3.6, dispersion 32 Å/mm. These and the photomultiplier were calibrated in terms of absolute transmission and spectral response by a Hilger Schwartz thermopile and a nanoammeter.

Frozen solutions in 2 mm Spectrosil tubes were prepared and degassed in a grease-free vacuum manifold. Excitation and emission spectra were measured in total immersion in liquid nitrogen in a Spectrosil dewar. Solvent purity was at least spectroquality.

The Raman spectrum of the crystal was obtained at 295 °K with a Perkin–Elmer LR1 Laser Raman spectrometer.

3. Molecular and Crystal Symmetry

From crystallographic studies(15) the molecular symmetry of HCB is believed to be the same as the parent, benzene, i.e. D_{6h}. However, studies of infrared(16,17) and ultraviolet(13) absorption spectra have suggested the molecule could be puckered. The displacement of the chlorine atoms out of the plane of the benzene ring would reduce the symmetry to D_{3d}.

HCB crystallizes in the monoclinic space group, $P2_1/c$ with two molecules per unit cell.(18) The crystal structure is summarized in Table 1. The squared direction cosines of the molecular axes with respect to the crystallographic axes are shown in Table 1 for the (001) and (100) planes. These were calculated from the molecular coordinates reported by Strel'tsova.(15)

Table 1 Hexachlorobenzene Crystal—Crystal Structure Data and Direction Cosines for the Orientation of the Molecular Axes with an Orthogonal Set of Crystal Axes

$P2_1/c$	*a*: 8.08 ± 0.02 Å β = 117.0° ± 0.2°		*b*: 3.87 ± 0.01 Å Z = 2		*c*: 16.65 ± 0.03 Å	
		ab plane			*bc* plane	
	a	*b*	*c**	*a**	*b*	*c*
L†	0.819	0.143	0.038	0.514	0.143	0.343
M	0.054	0.002	0.944	0.395	0.002	0.602
N	0.127	0.855	0.018	0.090	0.855	0.055

† Molecular axes: L axis bisects C–C bond, M is perpendicular to L in the plane of the molecule and passing through the C atom, and N is perpendicular to the molecular plane.

Designations in D_{6h} symmetry are $B_{1u}(M, y)$ and $B_{2u}(L, x)$.

4. Results and Discussion

4.1. Fluorescence Spectrum

The polarized $S_0 \rightarrow S_1$ absorption spectrum of single crystals at 4.2 °K was reported by Schnepp and Kopelman.(13) The electronic origin was assigned as 32735 cm^{-1}. They searched for, but could not observe, any fluorescence.

We have observed weak fluorescence from single crystals with a quantum yield $\phi_F \simeq 10^{-2}$. The polarized fluorescence spectrum from the *ab* face of a single crystal at 4.2 °K is shown in Fig. 1. The observed bands, their relative intensities, polarizations and assignments are summarized in Table 2.

On warming from 4.2 °K the bands broaden uniformly. There is no evidence for trapping levels (e.g. impurities or defects) below the exciton origin. This does not imply that the crystal is free from impurities or physical defects, but rather that the fluorescence spectrum is not sensitive to such traps. This would be expected for a weak $S_0 \rightarrow S_1$ transition (f $\simeq$ 0.002 from direct absorption spectra), since the appearance of trapped exciton origins requires not only the existence of sufficient concentration of defects but also the energy transfer to be rapid to these levels. The transfer of energy to traps is expected to be most rapid in strong electronic transitions.(10) For example, in anthracene crystals in which the oscillator strength for the first singlet transition is about 50 times larger than in HCB, the singlet exciton becomes trapped at defects and/or impurities. Anthracene crystal fluorescence at 4.2 °K has been recently assigned in terms of a number of origins corresponding to exciton traps ranging in depth from about 60 cm^{-1} to 1300 cm^{-1}.(19,20)

From the above observations we conclude that exciton fluorescence is being observed.

The first line observed in the spectrum is assigned as the electronic origin (32736 cm^{-1}). The transition $S_0 \rightarrow S_1$ ($^1A_{1g} \rightarrow {}^1B_{2u}$) is symmetry forbidden for a molecule of D_{6h} symmetry. The origin can be observed through crystal field effects.(13) In emission, the origin is polarized predominantly $\|$ *b*. From Table 1 this is seen to correspond to substantial out of plane intensity. This could be crystal field induced, or could result because the molecule is puckered to D_{3d} symmetry.

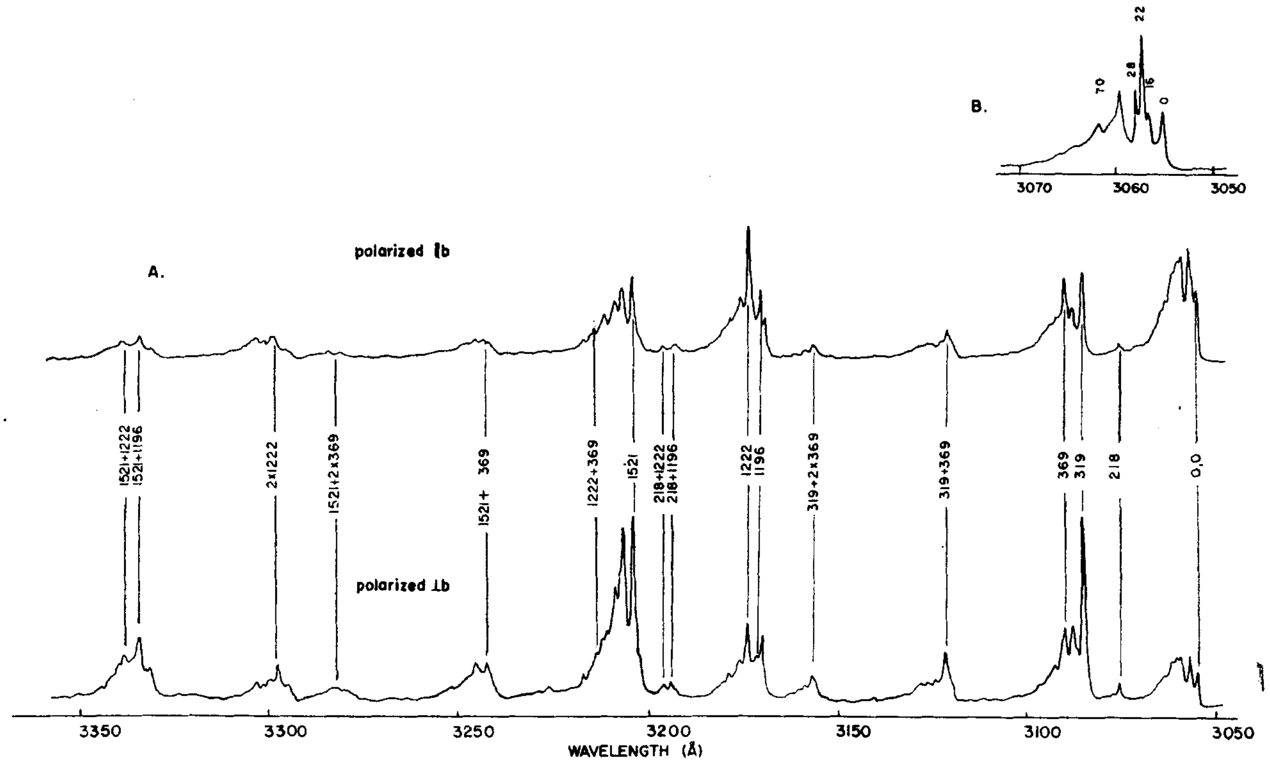

Figure 1. (A) Polarized fluorescence spectrum of hexachlorobenzene single crystal at 4.2 °K. (B) Phonon structure built on origin of fluorescence Unpolarized spectrum at 4.2 °K.

TABLE 2 Fluorescence Bands from Hexachlorobenzene Single Crystal at 4.2 °K

Relative intensity†	Polarization $I_{\parallel b}/I_{\perp b}$	$\tilde{\nu}$ (cm^{-1})	$\Delta\tilde{\nu}$	Assignment
s	2.3	32736	0	0–0
s		32720	16	16 lattice
vs	2.6	32714	22	22 lattice
s		32708	28	28 lattice
s	1.85	32690	46	2 × 22
s		32667	69	70 lattice
m		32643	93	70 + 22
m		32605	131	131 lattice
w	0.7	32518	218	218 e_{2g} fundamental
vw		32503	233	218 + 16
w		32444	292	218 + 70
s	0.5	32417	319	319 e_{2g} fundamental
s	0.65	32391	345	319 + 22 or 345 (e_{1g})
s	1.1	32367	369	369 a_{1g} fundamental
m	1.1	32342	394	369 + 22
w	0.6	32146	590	218 + 369
w	0.7	32051	685	319 + 369
w	0.7	32037	699	319 + 369 + 16
w	1.0	32013	723	319 + 369 + 28
w } diffuse		32005	731	2 × 369
vw		31988	748	2 × 369 + 16
vw		31957	779	2 × 369 + 28
vvw		31936	800	2 × 369 + 70
vw		31859	877	870 e_{2g} fundamental
w	0.5	31678	1058	319 + 2 × 369
vw		31653	1083	319 + 2 × 369 + 28
m	0.55	31554	1182	1182 e_{2g} fundamental
m	1.3	31540	1196	870 + 319 (e_{2g} + e_{2g})
s	2.0	31514	1222	1222 a_{1g} fundamental
m	1.6	31492	1244	1222 + 22
w	1.2	31464	1272	1222 + 22 + 28
w	1.1	31322	1414	218 + 1196
w	1.0	31293	1443	218 + 1222

Relative intensity†	Polarization $I_{\parallel b}/I_{\perp b}$	$\bar{\nu}$ (cm^{-1})	$\Delta\bar{\nu}$	Assignment
s	0.45	31215	1521	1521 e_{2g} fundamental
s	0.40	31189	1547	1521 + 22
m	0.5	31168	1568	1521 + 22 + 28
m	0.65	31145	1591	1521 + 70 or 1222 + 369
w		31120	1616	1521 + 70 + 22 or 1222 + 369 + 22
m	0.6	31091	1645	1521 + 130
w		31004	1732	1521 + 218
w		30984	1752	1521 + 218 + 16
w		30868	1868	1521 + 319 + 28
mw	0.45	30855	1881	1521 + 369
mw	0.45	30830	1906	1521 + 369 + 16
w		30769	1967	1521 + 369 + 70
vw		30721	2015	1521 + 369 + 130
w	0.5	30512	2224	
w	0.5	30486	2250	1521 + 2 × 369
w	1.65	30380	2356	
mw	0.9	30357	2379	1182 + 1196
mw	1.0	30350	2386	2 × 1196
mw	1.0	30304	2432	2 × 1222
w		30284	2452	2 × 1222 + 22
vw		30261	2475	2 × 1222 + 22 + 28
m	0.3	30066	2670	2 × 1222 + 219
m	0.4	30037	2699	2 × 1222 + 219 + 28
m	0.4	30022	2714	1521 + 1196
mw		29999	2737	1521 + 1222
w		29984	2752	1521 + 1222 + 16
w		29972	2764	2 × 1222 + 319
vw		29953	2783	2 × 1222 + 319 + 22
vw		29927	2809	2 × 1222 + 369
vw		29898	2838	2 × 1222 + 369 + 28
vw	0.6	29702	3034	1521 + 1196 + 319
vvw		29694	3042	2 × 1521
vw		29678	3058	2 × 1521 + 16
vw		29644	3092	2 × 1222 + (2 × 319)

† vs, very strong; s, strong; m, medium; w, weak; vw, very weak.

Intense bands corresponding to emission to levels of nontotally symmetric (e_{2g}) vibrations appear polarized $\perp b$. These carry the total vibronic symmetry to E_{1u} and are in-plane polarized. The two predominant bands of this type are at 319 cm^{-1} and 1521 cm^{-1} from the origin. Other similar but weaker bands are observed at 219 cm^{-1} (weak) and 877 cm^{-1} (very weak) from the origin. These also correspond to e_{2g} vibrations reported by Scherer and Evans.(17)

Two totally symmetric fundamentals 369 cm^{-1} and 1222 cm^{-1} are built on the origin and also appear in combination with the e_{2g} vibrations. The vibration at 1196 cm^{-1} polarized $\| b$ is interpreted as the combination 877 cm^{-1} (e_{2g}) + 319 cm^{-1} (e_{2g}) which gains intensity by Fermi resonance with the a_g fundamental 1210 cm^{-1}.(17) The band at 1182 cm^{-1} from the origin polarized $\perp b$ would appear to arise from a transition to an e_{2g} vibration level. No fundamental vibration of this magnitude has been reported. However, in absorption, an upper state frequency of 1149 cm^{-1} was observed by Schnepp and Kopelman.(13) This was assigned to an e_{2g} vibration. No strong progressions in the fluorescence are built on this origin (compared for example with the 1521 cm^{-1} e_{2g} fundamental).

In Table 3, the observed molecular vibrations from fluorescence of the crystal are compared with frequencies observed in the Raman spectrum of liquid HCB(17) and the crystal (this investigation). Each of the vibrations characterized in the Raman spectrum are also observed in fluorescence. The 340 cm^{-1} vibration interpreted as an e_{1g} mode in the Raman work could also be interpreted from the crystal fluorescence as (319 + 22) cm^{-1} since a lattice mode of 22 cm^{-1} is also recognized. We are unable to decide whether an e_{1g} mode at 340 cm^{-1} is active in the crystal fluorescence. Apart from this possible e_{1g} mode at 340 cm^{-1} there is no evidence for vibrations indicative of a puckered molecular configuration of HCB.

An expanded region of the origin is shown in Fig. 1 to indicate the phonon structure built on the origin. Substantial phonon structure can also be resolved in the vibrational structure. The lattice frequencies observed are listed in Table 3 and compared with the values observed in absorption. We have assigned the band at 130 cm^{-1} as a high lying lattice mode (or combination) rather than a b_{2g} vibration as proposed by Schnepp and Kopelman.

In a crystal of P$2_1/c$ symmetry with two molecules per unit cell,

TABLE 3 Molecular and Lattice Vibrations of Hexachlorobenzene

(a) Molecular vibrations (cm^{-1})

Symmetry	$\bar{\nu}$ (Raman solution)(17)	$\bar{\nu}$ (Raman crystal)‡	$\bar{\nu}$ (Fluorescence)	$\bar{\nu}$ ($S_0 \rightarrow T_1$)
A_{1g}	1210†	1228	1222	1189
	372	375	369	359
E_{2g}	1512	1520	1521	
	870		877	
	323	324	319	254
	219	219	218	195
E_{1g}	340	360	345	

(b) Lattice vibrations (cm^{-1})

Fluorescence	Phosphorescence	$S_0 \rightarrow T_1$ Absorption	$S_0 \rightarrow S_1$ Absorption
16	16	18	17(33)
22		24	22(13)
28	28	31	30(13)
70	74	73	
131	131	123	131(13,33)

† Corrected for Fermi Resonance.

‡ This investigation—Single Crystal.

there are six Raman active lattice vibrations each due to librational modes. Three of these vibrations are of A_g and three of B_g symmetry. For the D_{6h} molecular symmetry group, they belong to the representations of b_{2g}, b_{1g} and b_{3g}. We have recognized five of these vibrations from the fluorescence data but are unable to decide on the symmetry species of each lattice mode from our data.

4.2. PHOSPHORESCENCE SPECTRUM

Pure crystal phosphorescence is observed with a quantum yield $\phi_p \sim 10^{-2}$. The quantum yield is reduced from the frozen solution value because of triplet exciton quenching at the crystal surface. When strongly absorbed light is used (corresponding to the transition energies of the transitions $S_0 \rightarrow S_1$ or $S_0 \rightarrow S_2$) surface quenching can become a dominant radiationless process.(14)

Triplet exciton phosphorescence has an origin indicated by a weak band at 25685 cm^{-1}. From a comparison of the $S_0 \rightarrow T_1$ spectrum obtained in this study (see Sec. 4.3) and that of Marchetti and Kearns(9) this is assigned as the $T_1 \rightarrow S_0$ origin. Thus, in contrast to all previous reports of HCB phosphorescence there is *no* red shift between emission and absorption. Such an observation is expected for exciton phosphorescence and has been observed for the phosphorescence of *p*-dibromobenzene single crystals.$^{(1)}$

4.2.1. *Solution Phosphorescence Spectrum.* The emission spectrum of a ~10^{-4} M solution of HCB in 3-methyl pentane at 77 °K is shown in Fig. 2. This broad and structureless spectrum is identical to the

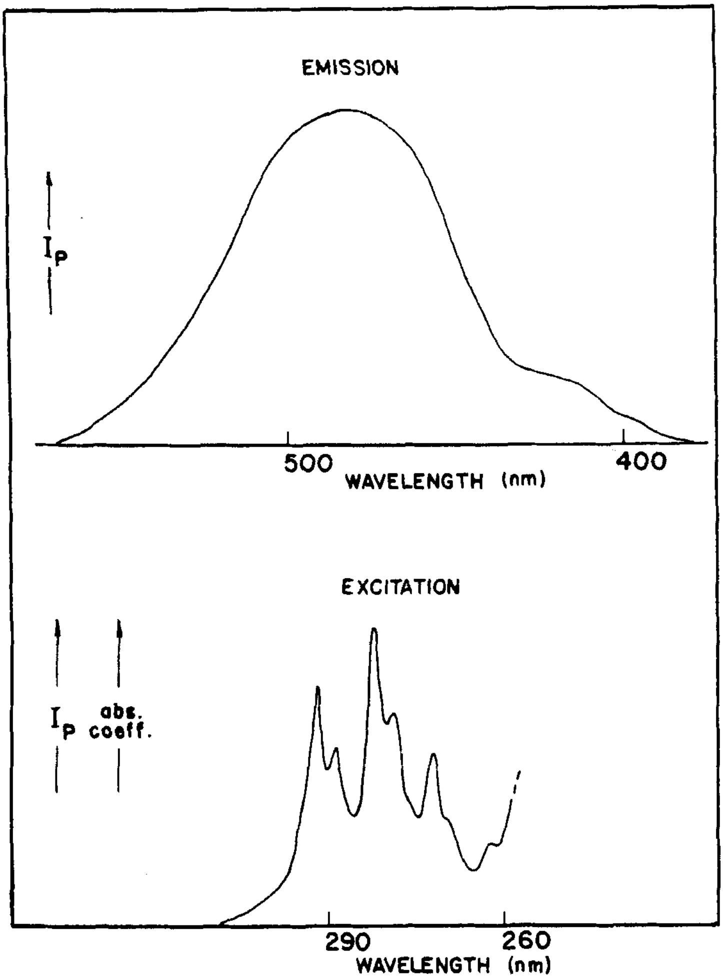

Figure 2. Phosphorescence emission and excitation spectra of a 10^{-4} M solution of hexachlorobenzene in 3-methyl pentane at 77 °K.

spectrum observed by Russell and Albrecht.(8) The excitation spectrum of the phosphorescence is shown also in Fig. 2. This is identical to the $S_0 \rightarrow S_1$ absorption spectrum in a frozen solution and indicates that the emission is characteristic of HCB and not due to impurities. Impurity effects are expected to be negligible in dilute frozen solution.

We believe the broad, structureless emission is explicable in terms of triplet excimer emission. Triplet excimer emission from halobenzene crystals(21) and frozen solutions of chlorinated benzenes(22) has been reported. In all cases the emission is broad and shifted by 4000–5000 cm^{-1} from the triplet absorption origin. Excimer emission from solution is generally only observed in concentrated solutions ($\sim 10^{-2}$ M). The observation of this emission in 10^{-4} M solution indicates that 3-methyl pentane at 77 °K must allow substantial rotation and migration of the HCB molecules to allow them to come into the most suitable configuration for formation of the excited dimer. When *n*-hexane or cyclohexane polycrystalline matrices are used, monomeric emission is predominant. The observed emission does not have bands as narrow as the quasi linear spectra obtained from aromatics in these solvents.(23) These cannot be good Shpol'skii solvents for HCB. With concentrations greater than 10^{-3} M, precipitation can occur (i.e. the formation of microcrystallites). The presence of microcrystallites can be detected from the excitation spectrum ($S_0 \rightarrow S_1$) of the phosphorescence. This now shows features characteristic of the crystal, namely antibatic behaviour with respect to the absorption spectrum.(14)

4.2.2. *Crystal Phosphorescence* 4.2 °K. The crystal phosphorescence spectrum is found to be very sensitive to the temperature of the crystal between 4.2 °K and 15 °K. At 4.2 °K the emission has an intense origin at 25646 cm^{-1}. From $S_0 \rightarrow T_1$ absorption studies (Sec. 4.3) we have assigned the triplet exciton origin at 25685 cm^{-1}. The emission at 4.2 °K cannot be the free triplet exciton phosphorescence. However, the spectrum (Fig. 3 and Table 4) can be assigned in terms of HCB molecular and lattice frequencies built on this origin. The emission presumably originates from a shallow exciton trap corresponding to a HCB molecule at a defect site. At this site, due to its perturbed surroundings, the triplet energy level of the molecule is about 39 cm^{-1} below the free triplet exciton band.

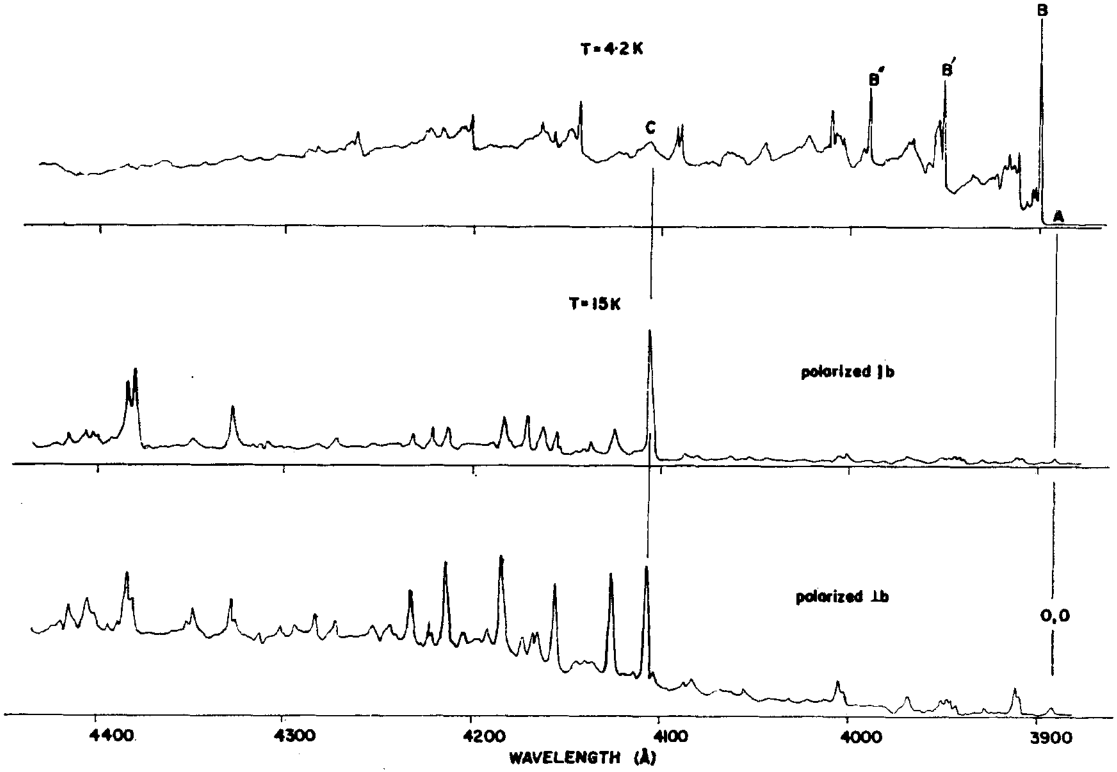

Figure 3. Phosphorescence spectrum of hexachlorobenzene single crystal at 4.2°K (unpolarized) and 15°K (polarized). (A, B, C are emission origins discussed in the text).

Whether the defect is caused by chemical impurities or is structural (dislocations, site vacancies, compressions, etc.) is not known. However, it is noteworthy that in this spectrum the background excimer emission is intense. Excimer emission in crystals has been considered to occur at a defect site or similar point in the crystal where translationally equivalent molecules can approach the most favourable configuration for excimer formation.(1) On this basis, it would appear that the shallow trap at 39 cm^{-1} may be structural in origin. If that is so, we would expect a number of such levels depending on the method of crystal preparation etc., and the temperature of observation. This is not observed and it would seem that chemical impurity induced defect centres may be important. The number of such trap levels active in the phosphorescence at 4.2 °K is difficult to ascertain with certainty. The phonon bands for this crystal are unknown and while our analysis of the observed bands uses only those lattice vibrations also observed in fluorescence, it is possible that some trap levels have been assigned as lattice modes. To be certain of our analysis, it is necessary to have measurements of both lattice vibrations and of phosphorescence band positions within accuracy of 1 cm^{-1}. Our measurement of band positions are accurate for the narrowest bands to 3 cm^{-1}, but for the more diffuse bands such errors could be as large at 8 cm^{-1}. Until more information is obtained, our assignments represent a consistent analysis.

In the spectrum there is a strong band at 25315 cm^{-1} with phonon structure built upon it. This band is 331 cm^{-1} from the emission origin. We have assigned this band as a transition from the defect energy level to a ground state vibrational level—probably an e_{2g} vibration (324 cm^{-1} in the Raman crystal spectrum). We note that this band at 25315 cm^{-1} is 370 cm^{-1} from the triplet exciton band. Whilst there is an a_{1g} ground state vibration of this magnitude, we know of no reason why such a vibration is observed when the emission from the triplet exciton origin is unobserved. Reabsorption of the emitted phosphorescence cannot explain the non-observance of the triplet exciton band origin. A further strong band at 25063 cm^{-1} (583 cm^{-1} from the defect origin) marks a transition to a ground state vibration level. This may be a ground state frequency of 583 cm^{-1} not previously observed or it could be a combination band 358 (a_{1g}) + 226 (e_{2g}). We believe it to be the latter.

TABLE 4 Phosphorescence Bands from Hexachlorobenzene Single Crystal at 4.2 °K

Relative intensity	Polarization $I_{\perp b}/I_{\parallel b}$	$\bar{\nu}$ (cm^{-1})	$\Delta\bar{\nu}$	Tentative assignment
vs	1.9	25646	0	Defect Origin
mw	2	25631	15	16 lattice
mw	1.5	25618	28	28 lattice
vw	~1	25600	46	16 + 28
vw		25595	51	2 × 28
m	3.7	25572	74	74 lattice
m	3.1	25555	91	74 + 16
m	3.5	25539	107	74 + 2 × 16
mw	3.5	25529	117	74 + 28 + 16
mw	2.3	25517	129	131 lattice
vw		25494	152	2 × 74
vw		25468	178	2 × 74 + 28
vw		25420	226	226 e_{2g} fundamental or 3 × 74
vw		25394	252	3 × 74 + 28
vw		25379	267	2 × 131
s	5.0	25315	331	331 e_{2g} fundamental
m	2.9	25299	347	331 + 16
mw		25288	358	358 a_{1g} fundamental or 331 + 28
w		25260	386	331 + 2 × 28
w		25240	406	331 + 74
m		25206	440	331 + 74 + 28
m		25192	454	331 + 131
s	6.0	25063	583	583 or 358 + 226
w		25046	600	583 + 16
mw		24980	666	583 + 74

Relative intensity	Polarization $\mathrm{I}_{\perp b}/\mathrm{I}_{\parallel b}$	$\bar{\nu}$ (cm^{-1})	$\Delta\bar{\nu}$	Tentative assignment
mw		24966	680	583 + 74 + 16
mw		24954	692	583 + 74 + 28
m		24941	705	583 + 131
w		24864	782	583 + 131 + 74
vw		24733	913	583 + 331
vw		24713	933	583 + 331 + 16
vw		24704	942	583 + 331 + 28
vvw		24680	966	583 + 331 + 2 × 28
vw		24480	1166	2 × 583
w		24462	1184	2 × 583 + 16
mw		24453	1193	2 × 583 + 16 + 28 or 1193
mw		24436	1210	2 × 583 + 2 × 16 + 28 or 1193 + 16
mw		24419	1227	a_{1g} fundamental
w		24348	1298	1227 + 74
vw		24162	1484	2 × 583 + 331
ms		24132	1514	e_{2g} fundamental
m		24109	1537	1514 + 28
w		24058	1588	1514 + 74
w		24023	1623	1514 + 74 + 28
vw		23913	1733	1514 + 226
w		23866	1780	583 + 1193
w		23858	1788	583 + 1193 + 16
w		23848	1798	583 + 1193 + 28
m		23798	1848	1514 + 331
mw		23771	1875	1514 + 331 + 28
mw		23760	1886	1514 + 358
mw		23548	2098	1514 + 358 + 226

The corresponding frequencies observed in the Raman spectrum are 375 cm^{-1} and 219 cm^{-1}.

Within the accuracy of the phosphorescence data there is a need to explain the variation of frequencies of the crystal ground state vibrations (e.g. 323, 375 cm^{-1}) to those observed (331, 358 cm^{-1}) in the defect phosphorescence spectrum. If the emission centres for phosphorescence are HCB molecules trapped near impurities as suggested, it is possible that these molecules are distorted. The internal force field is probably altered from that of the undistorted molecule. In this case a frequency variation of the magnitude observed is not surprising.

4.2.3. *Crystal Phosphorescence—Temperature Dependence.* Emission from the triplet exciton band is not observed until the crystal is warmed above 4.2 °K. The temperature dependence of the free triplet exciton origin region from 4.2 °K to 14 °K is shown in Fig. 4. As the temperature is increased the intensity of phosphorescence from the defect origin B decreases, and the background excimer emission in this region decreases. Also shown in Fig. 4 is the region $\sim$ 1345 cm^{-1} from the origin. As T increases, and the exciton origin A appears, so also does the narrow band C increase in intensity.

In Fig. 5 the inverse intensity of the peak B is plotted against inverse temperature. It is seen that the emission intensity follows an exponential relation of the form $1/I_p = C \exp(-\Delta E/kT)$. This leads to an activation energy, ΔE, of 41 cm^{-1} which is in excellent agreement with the trap depth of 39 cm^{-1} observed spectroscopically. As the temperature is increased above 4.2 °K, a trapped triplet exciton can be excited up to the intrinsic exciton band. Intrinsic phosphorescence of hexachlorobenzene may now be observed. The activation energy of 41 cm^{-1} confirms our assignment of the first triplet exciton band at 25685 cm^{-1}. Azumi and Nakano,$^{(24)}$ in a study of the defect phosphorescence of pyrazine, have observed the following temperature dependence

$$1/I_p = C_1 \exp(-\Delta E/kT) + C_2.$$

The observation of the low temperature inverse intensity limit (C_2) allows the trap density to be estimated. In hexachlorobenzene this limit presumably occurs below 4.2 °K, the lowest temperature of this

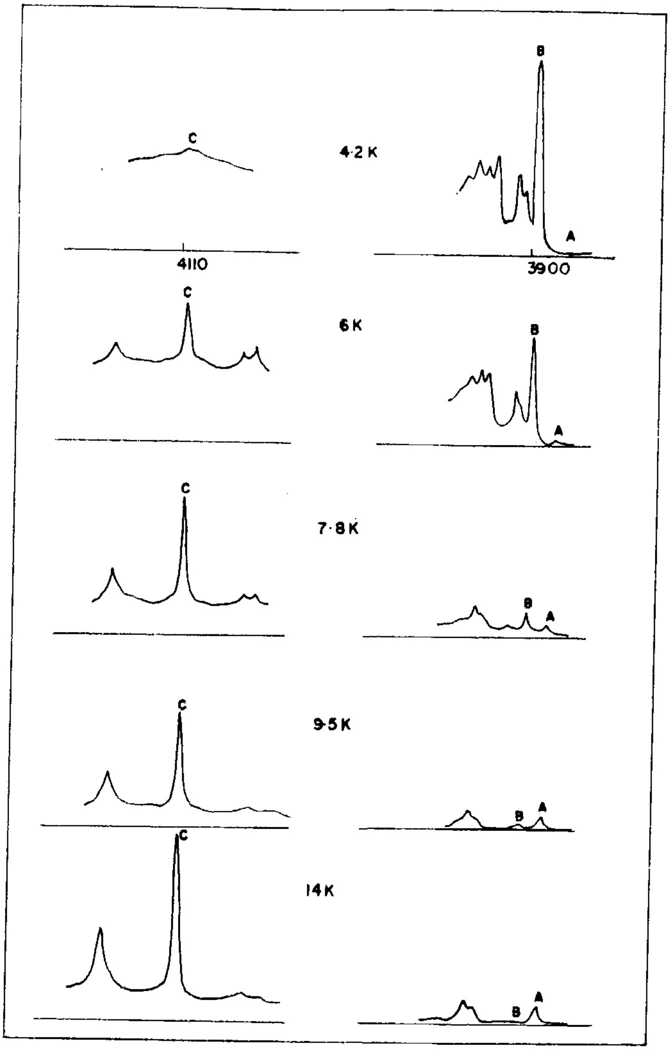

Figure 4. Variation with temperature of the phosphorescence intensity in the triplet exciton origin region and in the region 1345 cm^{-1} from the origin.

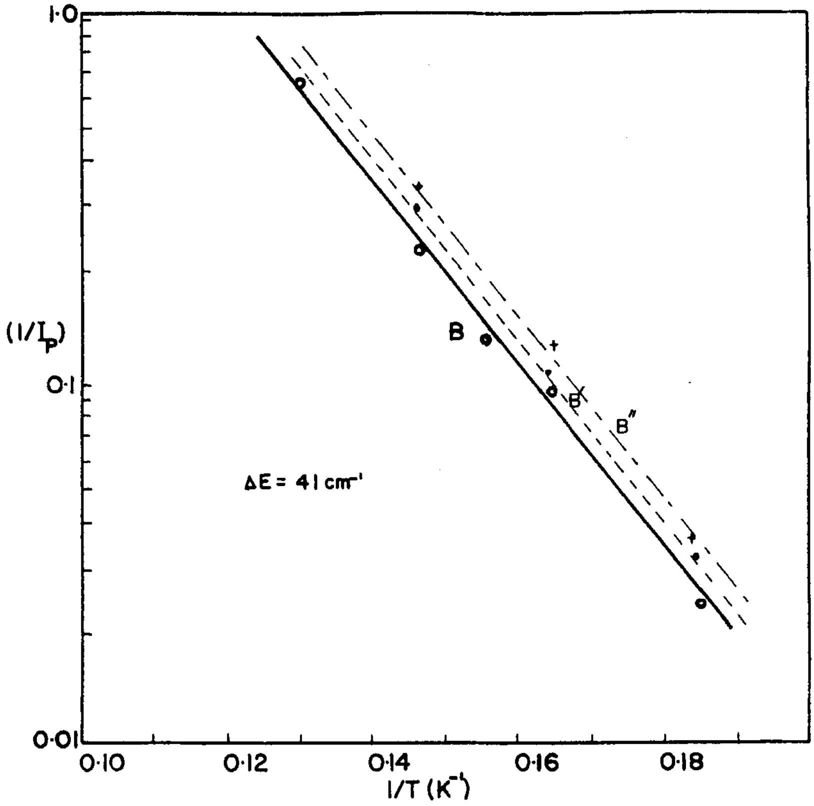

Figure 5. Dependence of the inverse phosphorescence intensity on the inverse temperature for the peaks B, B′, B″ of Figure 3.

investigation. Studies from 4.2 °K to 1 °K may enable a trap density to be estimated.

Also shown in Fig. 5 are the temperature variations of the peaks B′ and B″ of Fig. 3. These are seen to show the same activation energy as B. These emission peaks cannot be evidence for discrete trapping levels but must represent vibrational structure built on B.

In Fig. 6 is shown the variation of the full width at half maximum of peaks A and C from 5 °K to 40 °K. The width of peak A is seen to increase uniformly with temperature while peak C is unaltered. This is taken as evidence that the peak C may correspond to emission from a trapping level(19) as does peak B. We are not sure how these trapping levels arise. There is always the possibility of photo-

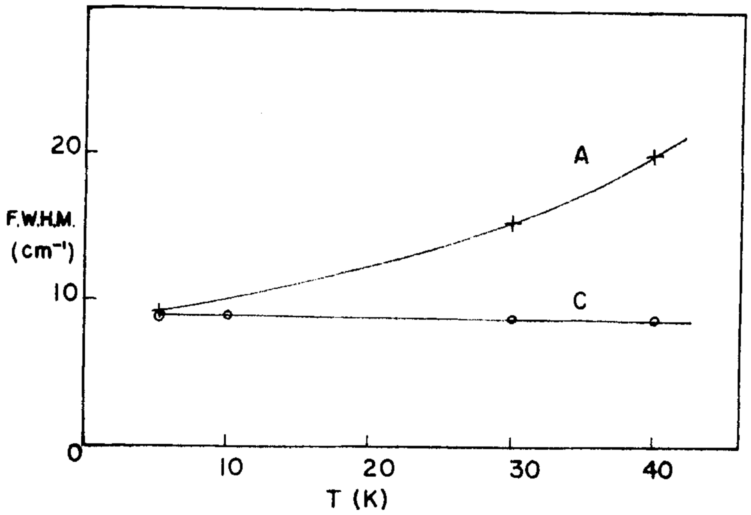

Figure 6. Temperature dependence of the full width at half maximum (FWHM) of the triplet exciton emission origin band (A) and of the false emission origin band (C).

chemical reaction during UV irradiation producing an impurity. However, spectra of crystals at 10 °K after prolonged irradiation and before irradiation were found to be identical. We also note that the displacement of peak C from the free triplet exciton emission origin (1345 cm^{-1}) corresponds to the frequency of the most intense IR active e_{1u} molecular vibration of HCB.(17) The appearance of such an ungerade mode in the emission spectrum is La Porte forbidden. However, Castro and Hochstrasser have observed b_{1u}, b_{3u} and a_u modes in the $S_0 \rightarrow T_1$ absorption spectra of the *p*-dihalobenzenes.(1) They have explained these as a consequence of higher order interactions involving intermediate states that do not combine with the ground state for dipole-allowed transition.

The polarized phosphorescence spectrum at 15 °K is shown in Fig. 3. Unlike the fluorescence spectrum or the " defect " phosphorescence spectrum an analysis in terms of molecular and lattice vibrations of hexachlorobenzene is not possible. While the band positions do not vary from sample to sample the relative intensity of bands originating from peak C and those from peak A vary from crystal to crystal. This is to be expected if the emission is sensitive to impurities and defects, since this depends on sample history. The bands which originate from the 1345 cm^{-1} trap mask any further emission that can be seen from the exciton origin.

The predominant polarization in the origin region is seen to be $\perp b$. The peak C is unpolarized. However, built on C are two progressions with different polarization properties. While certain molecular vibrations can be discerned a large number of peaks cannot be assigned. Lattice structure is not resolved (possibly a consequence of the higher temperature) and several origins (trapping levels) may be operative. This prevents any conclusive assignment of the spectrum.

We summarize the observed crystal phosphorescence spectrum as follows. At low temperatures $< 4.2\,°\text{K}$ the excitation energy is localized in traps close to the triplet exciton band. These traps are presumably HCB molecules whose triplet energy level has been displaced below the triplet exciton band by the presence of chemical impurities in the nearby lattice. They are probably not due to structural or lattice defects because in any batch of different crystals the spectrum is reproducible from crystal to crystal. We would expect that if the trapping level was induced due to lattice defects, it would alter from crystal to crystal and could possibly be annealed out. This has not been found. As the temperature increases above 4.2 °K, the triplet exciton band becomes thermally populated and triplet exciton emission is now observed. At the same time, band C also intensifies as the shallow traps are depopulated and the deep trap populated. If indeed C marks a trapping level, as seems likely, this would indicate that only a low concentration of such traps exist and that the mean free path of the triplet exciton increased with temperature. Under these conditions, most of the triplet excitons become localized in this deep trap which acts as the main emission level. This would explain why Olds(7) reported the crystal phosphorescence at 77 °K to originate entirely from this band. However, it is difficult to decide from what cause this trapping level arises. It would seem unlikely that shifting of the triplet energy level induced by impurities or crystal defects could be so large. A possibility is that the level is due to the presence of a chemical impurity. Certainly, the vibrational bands built on this level as origin do not bear a strong resemblance to the known molecular vibrations for the HCB molecule.

Finally we note that the phosphorescence spectrum is much more sensitive to defects and impurities than is the fluorescence spectrum. This is a reflection of the triplet exciton migration per triplet lifetime being more extensive than the singlet exciton migration per singlet lifetime.

4.3. SINGLET-TRIPLET ABSORPTION

The technique of phosphorescence excitation has been recently extended to enable high resolution $S_0 \rightarrow T_1$ spectra to be obtained at low temperatures.(25) This technique has certain advantages over direct absorption spectroscopy. Thin samples (of the order of 0.5 to 1 mm) only are required and samples may be cooled to 4.2 °K without cracking. In many cases because of the low efficiency of phosphorescence from pure aromatic molecular crystals, a suitable dopant with a lower triplet energy level than the host is used as a phosphorescent trap. However, pure crystal phosphorescence excitation spectra have an advantage over doped crystal excitation spectra for observation of triplet levels. There is no interference from the singlet state of the dopant and the triplet spectrum can be investigated to the onset of $S_0 \rightarrow S_1$ absorption. As a result the $S_0 \rightarrow T_2$ as well as the $S_0 \rightarrow T_1$ absorption can often be readily detected. A disadvantage is, however, the low intensity of emission from pure crystals so that a rather large spectral bandpass (4 to 5 cm^{-1}) has to be employed.

We have chosen to measure the excitation spectrum of the pure crystal phosphorescence.

4.3.1. *The First Triplet Exciton Band.* The polarized $S_0 \rightarrow T_1$ absorption spectrum of a *bc* oriented single crystal is shown in Fig. 7 and Table 5. Most of the intensity of the transition resides in the origin and the two a_g vibrations of 359 cm^{-1} and 1189 cm^{-1} (corresponding to vibrations of 372 cm^{-1} and 1210 cm^{-1} in the ground state —Table 3). Strong lattice structure is built on the origin band and on the totally symmetric vibrations. Lattice frequencies observed are summarized in Table 3 and compared with those obtained from the fluorescence spectrum. The remainder of the spectrum can be explained in terms of totally symmetric lattice and molecular modes built on two vibronic bands 195 cm^{-1} and 254 cm^{-1} from 0–0. The band at 254 cm^{-1} from the origin is polarized predominantly in-plane ($\perp b$) (as are the bands corresponding to the origin and a_g vibrations)

TABLE 5 $S_0 \rightarrow T_1$ Absorption Spectrum of Hexachlorobenzene Single Crystal at 4.2 °K

Relative intensity	Polarization *bc* plane I_c/I_b	 *ab* plane I_b/I_a	$\bar{\nu}$ (cm^{-1})	$\Delta\bar{\nu}$	Assignment
vs	1.9	0.4	25684	0	0, 0
vw	1.8	0.4	24702	18	18 lattice
vw			25708	24	24 lattice
vvw			25715	31	31 lattice
vvw			25724	40	24 + 18
vvw			25747	63	2 × 31
w	2.8	0.35	25757	73	73 lattice
vw			25764	80	2 × 31 + 18
vvw			25807	123	123 lattice
w			25825	141	123 + 18
mw	2.7	0.3	25832	148	2 × 73
vw	3.1	0.3	25865	181	2 × 73 + 31
m	1.0	1.2	25879	195	195 e_{2g} fundamental?
mw			25902	218	195 + 23
m			25931	247	195 + 23 + 31
m	2.6	0.2	25938	254	254 e_{2g} fundamental?
w	3.4	0.25	25964	280	254 + 23
vw			25994	310	254 + 23 + 31
s	1.9	0.5	26043	359	359 a_{1g} fundamental
w			26057	373	359 + 18
w			26077	393	359 + 31
w	2.0	0.5	26118	434	359 + 73
mw	2.0	0.5	26166	482	359 + 123
mw	2.1	0.4	26191	507	359 + 2 × 73
m	2.0	0.4	26221	537	359 + 2 × 73 + 31
mw	1.2	0.8	26241	557	195 + 359
m	2.2	0.3	26295	611	254 + 359
vw			26319	635	254 + 359 + 24
vw			26364	680	254 + 359 + 73
w	1.5	0.5	26400	716	2 × 359

Relative intensity	Polarization *bc* plane I_c/I_b	Polarization *ab* plane I_b/I_a	$\tilde{\nu}$ (cm^{-1})	$\Delta\tilde{\nu}$	Assignment
w			26414	730	$2 \times 359 + 16$
vw			26434	750	$2 \times 359 + 31$
vw			26480	796	$2 \times 359 + 73$
w			26522	838	$2 \times 359 + 123$
w			26550	866	$2 \times 359 + 2 \times 73$
w			26581	897	$2 \times 359 + 2 \times 73 + 31$
w			26607	923	$195 + 2 \times 359$
w			26649	965	$254 + 2 \times 359$
w			26770	1086	$254 + 2 \times 359 + 123$
s	1.9	0.4	26873	1189	1189 a_{1g} fundamental
w			26915	1231	$1189 + 31$
w			26944	1250	$1189 + 73$
w			27001	1317	$1189 + 123$
w	2.9	0.2	27018	1334	$1189 + 2 \times 73$
w	1.0	0.8	27067	1383	$195 + 1189$
mw	2.2	0.2	27122	1438	$254 + 1189$
w			27149	1454	$254 + 1189 + 31$
m	1.8	0.4	27229	1545	$359 + 1189$
w	1.9	0.4	27283	1599	$359 + 1189 + (31 + 23)$ or (2×31)
w			27374	1690	$359 + 1189 + 2 \times 73$
w			27412	1728	$195 + 359 + 1189$
vw	2.0	0.2	27487	1803	$254 + 359 + 1189$
vw			27593	1909	$2 \times 359 + 1189$
vw			27647	1963	$2 \times 359 + 1189 + 2 \times 31$
vw			27735	2051	$2 \times 359 + 1189 + 2 \times 73$
vw			27800	2116	
vw			27956	2272	
mw	1.8	0.4	28062	2378	2×1189
vw			28308	2524	$254 + 2 \times 1189$
vw			28413	2720	$359 + 2 \times 1189$
vw			28470	2786	$359 + 2 \times 1189 + 2 \times 31$
vw			28563	2879	

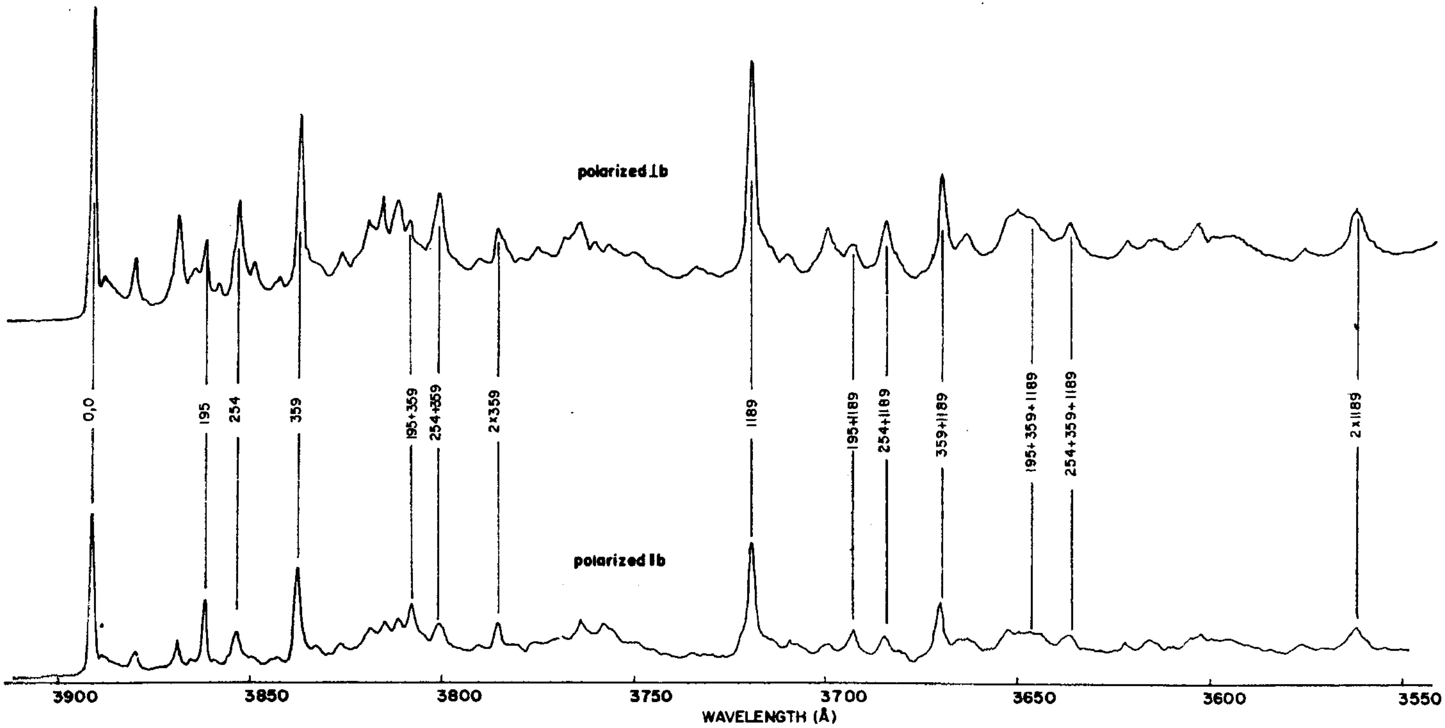

Figure 7. First singlet-triplet transition of hexachlorobenzene single crystal—polarized absorption spectrum at 4.2 °K by phosphorescence excitation.

while the band at 195 cm^{-1} shows more out-of-plane intensity. These bands could be related to the e_{2g} vibrations 323 cm^{-1} and 219 cm^{-1} (Table 3) except that they might be expected to show identical polarization behaviour. It is possible, when second order spin–orbit vibronic coupling routes are considered, that each e_{2g} vibration will not bring in comparable amounts of in-plane and out-of-plane polarized intensity. The vibration 219 cm^{-1} has been variously assigned as e_{1u}, e_{1g} and e_{2g}.(16,17,26) Scherer and Evans' calculations(17) confirm the symmetry to be e_{2g}, however.

No factor-group splitting was observed for the *ab* or *bc* faces. An estimate of the expected Davydov splitting of ~8 cm^{-1} has been made for HCB from triplet exciton diffusion studies.(14) This would be shared among the strong a_g vibrations. The origin bandwidth of ~10 cm^{-1} will also limit observation of any splitting.

4.3.2. *The Second Triplet Exciton Band.* A region of diffuse absorption is observed at 4.2 °K immediately before the onset of the absorption corresponding to the transition $S_0 \rightarrow S_1$. Only a broad shoulder and one peak can be resolved (see Fig. 8). By analogy

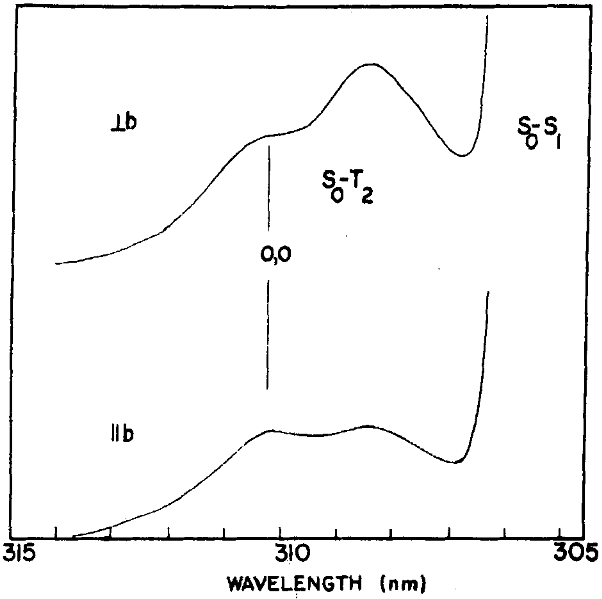

Figure 8. Second singlet triplet transition of hexachlorobenzene single crystal—polarized absorption spectrum at 4.2 °K by phosphorescence excitation.

with the corresponding transition observed in benzene,(27) this is assigned as the orbitally allowed, but spin forbidden, transition $^1A_{1g} \rightarrow {}^3E_{1u}$. The transition is observed to be polarized in-plane. The origin is located at 32240 cm^{-1} with a full width at half maximum of ~280 cm^{-1} at 4.2 °K. The effect of radiationless broadening of higher lying electronic states is seen in triplet as well as singlet states, e.g. the full width at half maximum of $S_0 \rightarrow T_1$ is only 10 cm^{-1}. We also note that the second triplet exciton band is ~500 cm^{-1} below the first singlet exciton band. Intersystem crossing to the triplet manifold would provide a highly competitive degradation route for the singlet exciton energy, as is borne out by the relatively low quantum yield of fluorescence.

5. Triplet State Symmetry

In planar aromatic molecules and also planar haloaromatics (e.g. halonaphthalenes) the origin region is polarized predominantly out of plane.(28) Direct spin–orbit interaction of $\pi\pi^*$ states with the $T \leftrightarrow S$ transition is vanishingly small and the only orbitals which have non-negligible overlap integrals are $\sigma\pi^*$, $\pi\sigma^*$, $\sigma\sigma^*$, $n\sigma^*$ and $n\pi^*$, all of which will bring out-of-plane intensity to the transition. The removal of planarity from the molecule will relax this requirement. Chaudhuri and El-Sayed(29) have shown that, in the origin region of the phosphorescence spectrum, naphthalene in durene shows substantial in-plane intensity while naphthalene in EPA or biphenyl shows mostly out-of-plane intensity. This is interpreted in terms of a change in hybridization of the molecule either from the crystal field of the durene or by forcing the guest to be slightly non-planar.

The $S_0 \rightarrow T_1$ transition of hexachlorobenzene in the crystal shows predominantly in-plane intensity (Table 5). In view of the significant crystal effects on the phosphorescence spectrum (as evidenced by the spectral temperature dependence) we shall initially consider only the information available from the $S_0 \rightarrow T_1$ absorption spectrum. To interpret the polarization data it is necessary to assume a particular spin–orbit coupling route. Albrecht in a study of benzene,(30) and Arden in a study of p-dichlorobenzene(31) have listed the spin–orbit coupling and spin–orbit vibronic coupling terms which contribute to the transition moment for the $S_0 \rightarrow T_1$ transition. The origin intensity will be expected to arise mainly from direct spin–orbit coupling of the triplet state to the singlet manifold. The singlet states considered will be those for which transitions from the ground state are symmetry allowed. Spin–orbit coupling of the ground state to the triplet manifold should formally also be considered. Goodman and Krishna have shown this coupling is significant for molecules with a large dipole moment(32) such as pyridazine. Coupling schemes involving the ground state will be of minor importance when a triplet state of high energy is being considered.

The predominantly in-plane intensity of the origin region for HCB cannot be explained by direct spin–orbit coupling within the framework of D_{6h} group symmetry of the molecule. However, a slight distortion of the molecule to D_{3d} symmetry will allow singlet states of symmetry $^1A_{2u}(z)$ and $^1E_u(x, y)$ to spin–orbit couple with the triplet state. Possible triplet states of symmetries $^3B_{1u}$ and $^3B_{2u}$ in D_{6h} group symmetry become states of symmetries $^3A_{2u}$ and $^3A_{1u}$ in D_{3d} group symmetry. The spin–orbit coupling operators transform as axial vectors in the appropriate space group, i.e. $A_{2g}(R_z)$ and $E_g(R_x, R_y)$ in D_{3d}. The selection rule requirement for a non-zero transition moment $\langle \psi(S_i) | H_{so} | \psi(T_1) \rangle \neq 0$, where S_i is the perturbing singlet state, leads to he conclusions

(i) a $^3A_{1u}$ state can spin–orbit couple with either an $^1A_{2u}$ state or an ^1E_u state to allow out-of-plane and in-plane absorption,

(ii) a $^3A_{2u}$ state can spin–orbit couple with an ^1E_u state only to allow in-plane absorption.

From Tables 5 and 1 the experimental and calculated (oriented gas) polarization ratios may be compared. The origin intensity in the *be* plane shows good agreement with the oriented gas value for a purely in-plane polarized transition. In the *ab* plane, however, some out-of-plane intensity is apparent. These results alone are not sufficiently conclusive to justify an asssignment of the triplet state as having either $^3A_{1u}$ or $^3A_{2u}$ symmetry.

The vibronic activity in the triplet absorption spectrum may arise through one or more of a number of mechanisms. Albrecht(27) has shown for benzene that the principal route involves vibronic coupling in the triplet manifold with spin–orbit coupling. If we consider the effect of a vibration of e_{2g} symmetry on the spin–orbit coupling selection rule it is found that polarization properties different from the origin should be observed viz.

$^3A_{1u}$: in-plane polarization only,
$^3A_{2u}$: in- and out-of-plane polarization.

From the $S_1 \rightarrow T_0$ absorption spectrum (Fig. 7, Table 5) the vibronic bands are of different polarization from the origin region. The 195 cm^{-1} vibration shows more out-of-plane intensity than the origin. If this corresponds to an e_{2g} mode the assignment of $^3A_{2u}(^3B_{1u})$ could be favoured. However, the polarization data is far from conclusive in view of the uncertainty of crystal field effects on the spectrum and the assumptions concerning the spin–orbit coupling route. Zeeman effect studies are the only conclusive experimental method⁽²⁾ for determining the precise route of spin–orbit coupling and the symmetry of the triplet state.

Acknowledgements

We thank the Australian Research Grants Committee for financial support and the Department of Supply (Aust.) for a Studentship (to G.A.G.).

REFERENCES

1. Castro, G. and Hochstrasser, R. M., *J. Chem. Phys.* **46,** 3617 (1967).
2. Castro, G. and Hochstrasser, R. M., *Mol. Cryst.* **1,** 139 (1966).
3. Castro, G. and Hochstrasser, R. M., *Solid State Commun.* **3,** 425 (1965).
4. Kasha, M., *Chem. Rev.* **41,** 401 (1947).
5. Pesteil, P., Pesteil, L. and Kara, R., *Compt. Rend.* **240,** 960 (1955).
6. Zmerli, A. and Pesteil, P., *Compt. Rend.* **240,** 2217 (1955).
7. Olds, D., *J. Chem. Phys.* **35,** 2248 (1961).
8. Russell, P. G. and Albrecht, A. C., *J. Chem. Phys.* **41,** 2536 (1964).
9. Marchetti, A. and Kearns, D. R., *J. Am. Chem. Soc.* **89,** 768 (1967).
10. Craig, D. P. and Walmsley, S. H., " Excitons in Molecular Crystals ", Benjamin, N.Y. (1968).
11. Logan, L. M., Munro, I. H., Williams, D. F. and Lipsett, F. R., in " Molecular Luminescence ", ed. E. C. Lim, Benjamin, N.Y. (1969).
12. Clarke, R. H. and Hochstrasser, R. M., *J. Chem. Phys.* **46,** 4532 (1967); Padhye, M. R., McGlynn, S. P. and Kasha, M., *J. Chem. Phys.* **24,** 588 (1956).
13. Schnepp, O. and Kopelman, R., *J. Chem. Phys.* **30,** 868 (1959).
14. George, G. A. and Morris, G. C., *Mol. Cryst. and Liq. Cryst.* In the press.

15. Strel'tsova, N. and Struchkov, Yu. T., *J. Struct. Chem.* **2**, 296 (1961).
16. Delorme, P., Denisselle, F., and Lorenzelli, V., *J. Chim. Phys.* **64**, 591 (1967).
17. Scherer, J. R. and Evans, J. C., *Spectrochim. Acta.* **19**, 1739 (1963).
18. Lonsdale, K., *Proc. Roy. Soc. A.* **133**, 536 (1931).
19. Glockner, E. and Wolf, H. C., *Zeit. f. Natur.* **24a**, 943 (1969); Lyons, L. E. and Warren, L. J. To be published.
20. Morris, G. C., Rice, S. A. and Martin, A. E. To be published.
21. Castro, G. and Hochstrasser, R. M., *J. Chem. Phys.* **45**, 4352 (1966).
22. Lim, E. C. and Chakrabarti, S. K., *Mol. Phys.*, **13**, 293 (1967); Chakrabarti, S. K., *Mol. Phys.* **16**, 417 (1969).
23. Shpol'skii, E. V., *Soviet Physics Uspekhi* **6**, 411 (1963).
24. Azumi, T. and Nakano, Y., *J. Chem. Phys.* **51**, 2515 (1969).
25. Castro, G. and Robinson, G. W., *J. Chem. Phys.* **50**, 1159 (1969).
26. Saeki, S., *Bull. Chem. Soc. Japan* **35**, 322 (1962).
27. Colson, S. D. and Bernstein, E. R., *J. Chem. Phys.* **43**, 2661 (1965).
28. El-Sayed, M. A., *Acc. Chem. Res.* **1**, 8 (1968).
29. Chaudhuri, N. K. and El-Sayed, M. A., *J. Chem. Phys.* **43**, 1423 (1965).
30. Albrecht, A. C., *J. Chem. Phys.* **38**, 354 (1963).
31. Arden, R. C., Ph.D. Thesis, University of Pennsylvania (1967).
32. Goodman, L. and Krishna, V. G., *J. Chem. Phys.* **37**, 2721 (1962).
33. Pesteil, P., Shurvell, H. F. and Pesteil, L., *Can. J. Chem.* **43**, 3133 (1965).